

**$^{22}\text{Ne}(d, \alpha)^{20}\text{F}$  reaction\***

H. T. Fortune and J. D. Garrett<sup>†</sup>

*Physics Department, University of Pennsylvania, Philadelphia, Pennsylvania 19174*

(Received 11 March 1976)

The reaction  $^{22}\text{Ne}(d, \alpha)^{20}\text{F}$  has been studied at a bombarding energy of 10.0 MeV, and excitation energies 0–7 MeV. Within the resolution of 24 keV, the reaction populates all known states below 6 MeV in excitation and four new states at 4.372, 4.518, 5.131, and 5.574 MeV. Angular distributions from 15° to 152.5° (lab) have been extracted for all states below 4.4 MeV, and integrated to get total cross sections. A large compound-nucleus component is present for all states. In addition, states expected to have a large direct-pickup cross section are observed to have a measurable direct component.

NUCLEAR REACTIONS  $^{22}\text{Ne}(d, \alpha)$ ,  $E = 10$  MeV; measured  $\sigma(\theta)$ , integrated  $\sigma$ .  
 $^{20}\text{F}$  levels, 0–7 MeV. Enriched target, DWBA analysis of integrated  $\sigma$ , resolution 24 keV;  $\theta = 15$ –152.5°,  $\Delta\theta = 7.5$ °.

**I. INTRODUCTION**

The reaction  $^{22}\text{Ne}(d, \alpha)^{20}\text{F}$  has been used to investigate the bound states of  $^{20}\text{F}$  up to 7 MeV excitation. It was expected that the reaction mechanism would be dominantly compound and that most states would be populated nonselectively. The reaction would then be an excellent way of producing all the  $T = 1$  states in  $^{20}\text{F}$ .

**II. EXPERIMENTAL PROCEDURE**

The reaction was initiated by a beam of 10.0-MeV deuterons from the Penn tandem. Outgoing  $\alpha$  particles were momentum analyzed in a multi-angle spectrograph and stopped in nuclear track plates. The target consisted of 19.5 Torr (cor-

responding to an areal density of 21.7  $\mu\text{g}/\text{cm}^2$ ) of  $^{22}\text{Ne}$  gas (enrichment = 99.8%) contained in a gas cell with no entrance window.<sup>1</sup> The gas was circulated and purified as described elsewhere.<sup>2</sup> The outgoing  $\alpha$  particles exited through a 175- $\mu\text{g}/\text{cm}^2$  window made<sup>3</sup> of Paralyne C. Typical resolution was 24 keV full width at half maximum. The absolute cross section scale was established from the known gas pressure and gas cell geometry, and is accurate to  $\pm 20\%$ .

Data were collected simultaneously at 21 angles from 7.5° to 152.5° in steps of 7.5°. For states below  $E_x = 4.4$  MeV, data were analyzed for all angles from 15° to 152.5°, but only the data for angles 15°–90° were used in the calculation of excitation energies because the spectrograph calibration is not accurately enough known at

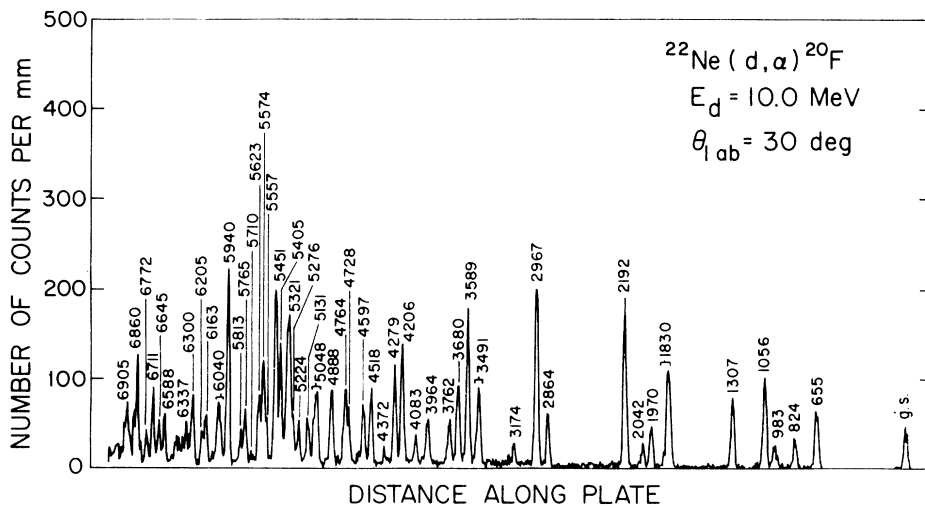


FIG. 1.  $\alpha$ -particle spectrum corresponding to the reaction  $^{22}\text{Ne}(d, \alpha)^{20}\text{F}$  measured at an incident energy of 10 MeV and at a laboratory angle of 30°.

TABLE I. Results of the  $^{22}\text{Ne}(d, \alpha)^{20}\text{F}$  reaction at  $E_d = 10.0$  MeV.

Literature <sup>a</sup>	Present	$\frac{\sigma_{\text{TOT}}(\mu\text{b})}{0-180^\circ}$	$\frac{\sigma_{90-180^\circ}}{\sigma_{90-180^\circ}}$	$\frac{\sigma_{\text{TOT}}(\mu\text{b})}{2J+1}$	b	Model <sup>c</sup>	$\frac{\sigma_{\text{th}}(\mu\text{b})}{2J+1}$	$N^d$	Comment
$E_x$ (MeV)	$E_x$ (MeV $\pm$ keV)	$0-180^\circ$	$90-180^\circ$	$2J+1$	$\sigma_{\text{th}} (\mu\text{b})$	state	$\frac{\sigma_{\text{th}}(\mu\text{b})}{2J+1}$		
0.000	...	858 $\pm$ 18	0.97 $\pm$ 0.04	171.7 $\pm$ 3.6	0.40	2 $_1^+$	0.080	380	
0.656	0.655 $\pm$ 2	2203 $\pm$ 29	1.01 $\pm$ 0.03	314.8 $\pm$ 4.2	4.10	3 $_1^+$	0.59	300	
0.823	0.824 $\pm$ 3	1508 $\pm$ 24	0.79 $\pm$ 0.03	167.6 $\pm$ 2.7	0.20	4 $_1^+$	0.022	1380	
0.984	0.983 $\pm$ 3	655 $\pm$ 15	0.87 $\pm$ 0.05	218.4 $\pm$ 5.0					
1.057	1.056 $\pm$ 4	1261 $\pm$ 22	1.37 $\pm$ 0.03	420.2 $\pm$ 7.2	2.3	1 $_1^+$	0.76	370	
1.309	1.307 $\pm$ 3	1290 $\pm$ 21	1.58 $\pm$ 0.03	258.0 $\pm$ 4.3					
1.824	1.830 $\pm$ 7	3276 $\pm$ 39	1.42 $\pm$ 0.02	204.7 $\pm$ 2.5	2.3	5 $_1^+$	0.21	470	
1.843									
1.971	1.970 $\pm$ 4	770 $\pm$ 16	1.15 $\pm$ 0.04	110.1 $\pm$ 2.4					
2.044	2.042 $\pm$ 3	685 $\pm$ 16	1.20 $\pm$ 0.04	137.0 $\pm$ 3.1	0.86	2 $_2^+$	0.17	60	
2.195	2.192 $\pm$ 3	1936 $\pm$ 27	2.10 $\pm$ 0.03	276.6 $\pm$ 3.9	2.4	3 $_2^+$	0.35	410	
2.865	2.864 $\pm$ 3	962 $\pm$ 18	1.27 $\pm$ 0.04	137.4 $\pm$ 2.6					
2.966	2.967 $\pm$ 3	2764 $\pm$ 33	1.16 $\pm$ 0.02	172.8 $\pm$ 2.1	1.5	3 $_3^+$	0.21	380	
3.175	3.174 $\pm$ 3	358 $\pm$ 11	2.51 $\pm$ 0.09	119.5 $\pm$ 3.6		1 $_3^+$ f	0.71	< 0	g
3.488	3.491 $\pm$ 4	1210 $\pm$ 20	1.58 $\pm$ 0.04	302.4 $\pm$ 5.0	1.3	1 $_2^+$	0.44	510	
3.526									
3.587	3.589 $\pm$ 3	2381 $\pm$ 30	1.21 $\pm$ 0.02		1.6	2 $_3^+$ f		1060	h
					1.5	3 $_3^+$ f		950	h
3.681	3.680 $\pm$ 3	1598 $\pm$ 23	1.30 $\pm$ 0.03		0.098	4 $_2^+$ f		3740	i
3.761	3.762 $\pm$ 4	1303 $\pm$ 21	1.18 $\pm$ 0.03						
3.966	3.964 $\pm$ 4	608 $\pm$ 14	1.98 $\pm$ 0.05		0.71	1 $_3^+$	0.24	290	j
4.082	4.083 $\pm$ 4	823 $\pm$ 16	1.58 $\pm$ 0.04	274.4 $\pm$ 5.5	0.71	1 $_3^+$		620	k
4.199	4.206 $\pm$ 4	2061 $\pm$ 28	1.99 $\pm$ 0.03						
4.208									
4.277	4.279 $\pm$ 4	1330 $\pm$ 20	2.26 $\pm$ 0.04						
4.312	4.372 $\pm$ 4	360 $\pm$ 11	1.04 $\pm$ 0.06						

<sup>a</sup> As summarized in Refs. 5, 9, and 10.

<sup>b</sup> Integrated predicted direct reaction cross sections based on shell-model wave functions—see text.

<sup>c</sup> Shell-model state with which this state is identified for calculation of  $\sigma_{\text{th}}$ .  $J^\pi$  designates  $i_{\text{th}}$  state of spin-parity  $J^\pi$  from shell model.

<sup>d</sup> DWBA normalization constant extracted using  $N = [10 \sigma_{\text{TOT}} - 137(2J+1)]/\sigma_{\text{th}}$ .

<sup>e</sup> Suggested from  $2J+1$  rule and weak ( $d, \alpha$ ) cross section.

<sup>f</sup> Trial identification for calculation of  $\sigma_{\text{th}}$  not suggested previously by experimental studies. A value for  $N \approx 330 \pm 80$  for a state predicted to have a large direct reaction cross section indicates a possible association of this state with the predicted shell-model state.

<sup>g</sup> Too weak to be associated with the predicted  $1\frac{1}{2}^+$  shell-model state.

<sup>h</sup> Too strong for identification with either  $2\frac{3}{2}^+$  or  $3\frac{3}{2}^+$ .

<sup>i</sup> Reasonable identification because predicted direct reaction cross section is so small.

<sup>j</sup> Reasonable strength to be associated with  $1\frac{1}{2}^+$ .

<sup>k</sup> Too strong to be the  $1\frac{1}{2}^+$  model state.

the back angles. The large background of low-energy continuum deuterons at forward angles made it extremely difficult to scan the  $7.5^\circ$  plate for  $\alpha$  particles. Thus, data at  $7.5^\circ$  were obtained for only a few selected states.  $\alpha$ -particle groups corresponding to states above 4.4 MeV were off the plate at back angles (because of kinematics), and, consequently, complete angular distributions could not be obtained for them. However, the region of excitation 4.4–7.0 MeV was scanned at enough angles ( $15^\circ$ – $45^\circ$ ) to allow extraction of reliable excitation energies. A typical spectrum is displayed in Fig. 1. The complete absence of contaminant peaks in the spectrum caused us to rely on the absolute spectrograph calibration<sup>4</sup> and the published<sup>5</sup>  $^{22}\text{Ne}(d, \alpha)^{20}\text{F}$  ground-state  $Q$  value ( $Q=2.701$  MeV) to obtain excitation energies. The excitation energies are listed in Tables I and II. Our energies are in reasonable agreement with those in a recent compilation,<sup>5</sup> but our results are not nearly as accurate. A correction has been made for the energy loss of the  $\alpha$  particles

in the exit window.

Because of the poor (24 keV) resolution inherent in gas-cell experiments with low-energy exiting  $\alpha$  particles, it is likely that many of the “levels” reported here actually consist of two or more levels. In fact, in some cases, our resolution is not sufficient to completely resolve previously known<sup>5</sup> doublets.

Within our resolution, all states previously<sup>5</sup> known below 6 MeV in  $^{20}\text{F}$  are observed to be populated in the  $^{22}\text{Ne}(d, \alpha)^{20}\text{F}$  study. Below 6 MeV in excitation, there are nine closely spaced doublets and one triplet. They are at excitation energies of 1.824–1.843, 2.966 (separation unknown), 3.488–3.526, 4.199–4.208, 4.277–4.312, 4.584–4.592, 4.892–4.898, 5.040–5.066, 5.317–5.344, and 5.450–5.455–5.463. Of these, even with our 24-keV resolution, we can state definitely that both members of five doublets are populated (those at 1.8, 3.5, 4.3, 5.0, and 5.3 MeV) and at least two members of the 5.4-MeV triplet are populated. We cannot state that both members of

TABLE II. Excitation energies (MeV  $\pm$  keV) for levels above 4.4 MeV.

Literature <sup>a</sup>	Present	Literature <sup>a</sup>	Present
...	4.518 $\pm$ 4	...	6.337 $\pm$ 5
4.5838 $\pm$ 3.0	4.597 $\pm$ 4	...	6.370 $\pm$ 6
4.5922 $\pm$ 2.9		...	6.407 $\pm$ 12
4.7302 $\pm$ 2.9	4.728 $\pm$ 8	...	6.441 $\pm$ 9
4.7638 $\pm$ 2.7	4.764 $\pm$ 7	...	6.480 $\pm$ 5
4.8916 $\pm$ 2.8	4.888 $\pm$ 4	6.513 $\pm$ 33 <sup>b</sup>	...
4.8982 $\pm$ 2.8		6.6013 $\pm$ 0.3	6.588 $\pm$ 5
5.0402 $\pm$ 3.1	5.048 $\pm$ 4	6.616	
5.0655 $\pm$ 3.1		6.627	
...	5.131 $\pm$ 5	6.634	
5.2240 $\pm$ 3.1	5.224 $\pm$ 6	6.637	
5.2810 $\pm$ 3.3	5.276 $\pm$ 5	6.648	6.645 $\pm$ 5
5.3171 $\pm$ 2.7	5.321 $\pm$ 4	6.668	
5.3445 $\pm$ 3.3		6.685	
5.4131 $\pm$ 0.6	5.405 $\pm$ 5	6.692	
5.4503 $\pm$ 3.8	5.451 $\pm$ 5	6.696	
5.4554 $\pm$ 3.2		6.699	
5.4634 $\pm$ 3.3		6.709	6.711 $\pm$ 5
5.5547 $\pm$ 0.6	5.557 $\pm$ 5	6.717	
...	5.574 $\pm$ 6	6.729	
5.6203 $\pm$ 3.3	5.623 $\pm$ 4	6.732	
(5.713 $\pm$ 2)	5.710 $\pm$ 11	6.737	
5.7628 $\pm$ 3.4	5.765 $\pm$ 3	6.742	
5.8091 $\pm$ 2.9	5.813 $\pm$ 4	6.746	
5.9361 $\pm$ 0.3	5.940 $\pm$ 5	6.791	6.772 $\pm$ 6
6.0173 $\pm$ 0.3	6.040 $\pm$ 4	6.835	
6.0446 $\pm$ 0.4		6.837	
...	6.163 $\pm$ 6	6.856	
...	6.205 $\pm$ 6	6.858	6.860 $\pm$ 13
6.25 $\pm$ 20	6.240 $\pm$ 7		6.905 $\pm$ 8
...	6.300 $\pm$ 5	7.005	

<sup>a</sup> See Ref. 5.

<sup>b</sup>  $T=2$ .

the 2.97-, 4.2-, 4.6-, and 4.9-MeV doublets are populated, but we suspect that they are. Four previously unreported states were observed at  $E_x=4.372$ , 4.518, 5.131, and 5.574 MeV. These levels were first observed in an earlier study<sup>6</sup> of the  $^{22}\text{Ne}(d, \alpha)^{20}\text{F}$  reaction and have subsequently been reported in a study of the  $^{14}\text{N}(^7\text{Li}, p)^{20}\text{F}$  reaction.<sup>7</sup> Several new states are observed above 6 MeV. However, we fail to observe many of the previously reported levels between 6.60 and 6.86 MeV. We suspect that many of them do not exist.

A state at 5.713 MeV listed as doubtful in the compilation is probably the state we see at 5.710 MeV.

### III. RESULTS

Angular distributions for all states below 4.4 MeV are displayed in Fig. 2. They are generally

featureless, with approximate symmetry about  $90^\circ$ , as expected for a reaction that is dominantly compound. Integrated cross sections

$$\sigma_{\text{TOT}} = 2\pi \int_{\theta_{\text{min}}}^{\theta_{\text{max}}} \sigma(\theta) \sin\theta d\theta$$

have been obtained and are also listed in Table I. The yield has been integrated separately forward and backward of  $90^\circ$ ; their ratios are also given in the table. In earlier studies<sup>8</sup> of  $(d, \alpha)$  reactions on light nuclei, but at somewhat lower energies, it was found that the total cross section leading to a given final state of spin  $J_f$  was roughly proportional to  $2J_f + 1$ . The ratio of the integrated cross sections divided by  $2J + 1$  is given in Table I for all states in  $^{20}\text{F}$  of known<sup>5,9,10</sup>  $J^\pi$ . The values of this ratio fall into two rather distinct groups: those for which  $\sigma_{\text{TOT}}/(2J + 1) \approx 160 \pm 50$  and those

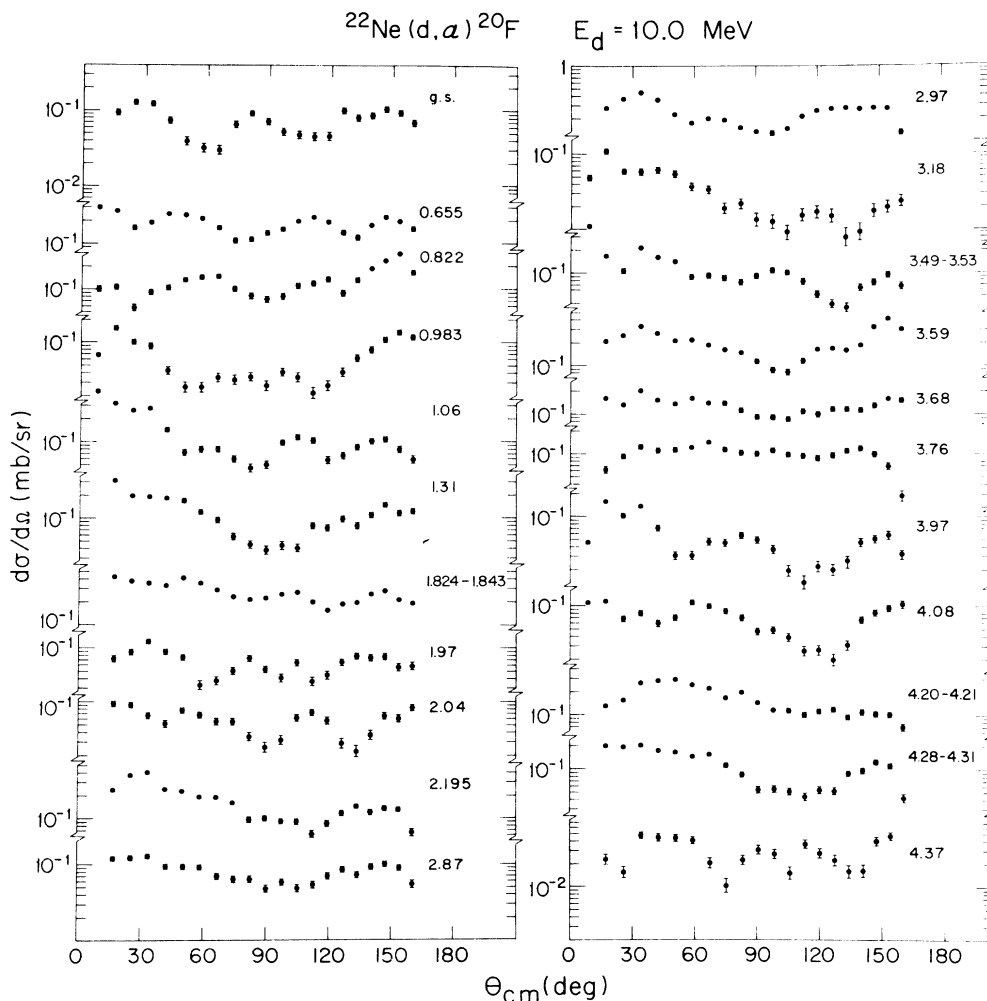


FIG. 2. Angular distributions corresponding to the reaction  $^{22}\text{Ne}(d, \alpha)^{20}\text{F}$  at an incident energy of 10 MeV. The error flags shown on the data points correspond to statistical errors and uncertainties in extracting the yield for certain closely spaced levels.

with significantly larger values of this ratio. The states at 0.66, 1.06, 1.31, 2.19, 3.49, and 4.08 MeV in excitation, e.g., would be in the latter group. Thus, the reaction has a large compound component as expected. However, for certain states, an appreciable noncompound component appears also to be present. On the basis of their small total cross sections, states at 3.18, 3.97, and 4.37 MeV probably have low spin,  $J=0$  or 1. The cross section for the 3.68-MeV state is consistent with its suggested<sup>10</sup>  $4^+$  assignment.

We can try to understand the enhanced cross sections for some of the other states by making use of two-particle transfer amplitudes<sup>11</sup> from a shell-model calculation.<sup>12</sup> In a model<sup>12</sup> that assumes a closed  $^{16}\text{O}$  core and allows particles to occupy the  $1d_{5/2}$ ,  $2s_{1/2}$ , and  $1d_{3/2}$  orbitals, the properties of all known positive-parity levels below 4 MeV in  $^{20}\text{F}$  are reasonably well described.<sup>9,10,12</sup> This model also provides an adequate description<sup>13</sup> of the ground state of  $^{22}\text{Ne}$ . We have used two-nucleon-transfer amplitudes from this shell-model calculation<sup>11</sup> as input to the code DWUCK<sup>14</sup> in order to estimate the expected direct cross sections. Distorted-wave Born-approximation (DWBA) treatment of  $(d, \alpha)$  reactions at such low energies is, of course, highly suspect. We have not tried to fit any angular distributions; we simply use the DWBA results as a qualitative guide to the strengths expected from the direct component for certain states. Predicted shapes of  $L=0, 2, 4$  transfer for one set of optical-model parameters<sup>15,16</sup> (deuteron set 7 of Ref. 15, and the  $\alpha$  potential of Ref. 16) are shown in Fig. 3. These shapes are not stable against changes in the parameters, and the predicted shapes for large values of the transferred

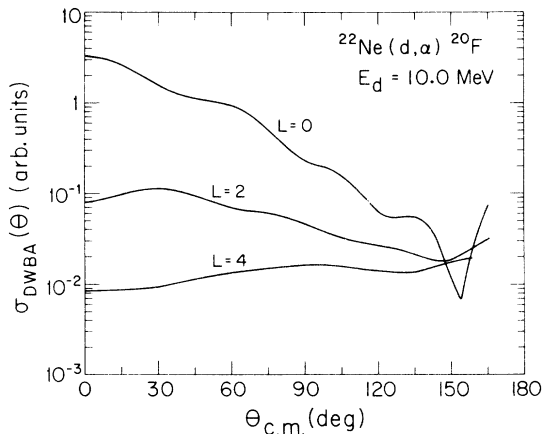


FIG. 3. Predicted angular shapes of pure  $L=0, 2,$  and  $4$   $^{22}\text{Ne}(d, \alpha)^{20}\text{F}$  transitions at an incident deuteron energy of 10 MeV. The optical-model parameters are from Refs. 15 and 16.

angular momenta  $L$  are not forward peaked. Thus in what follows, we make use only of the predicted total cross sections. In Table I the angle-integrated cross sections from DWUCK are listed for certain of the low-lying positive-parity states. The identifications of specific experimental states with shell-model counterparts are as summarized in Ref. 10 or discussed below. In general, the states that are predicted to be strong are those that are observed experimentally to have larger cross sections than explained by the  $2J+1$  rule. For example, the direct pickup cross section for the 0.66-MeV state is predicted to be 10 times that for the ground state. Indeed, the 0.66-MeV state has an integrated cross section that is consistent with a sizable direct component, whereas all of the ground-state cross section could be explained by a compound process. Similarly, a large direct pickup is predicted and observed for the 1.06-MeV  $1^+$  state.

If we make the naive assumptions that (1) the total cross section is simply the sum of the compound and direct-pickup cross sections, (2) the compound cross section is proportional to  $(2J+1)$  i.e.,  $\sigma_{\text{CN}} = \sigma_{\text{C}}(2J+1)$ , where  $\sigma_{\text{C}}$  is independent of spin, parity, and excitation energy, and (3) the direct-pickup total cross section  $\sigma_{\text{p.u.}}$  is adequately described by DWBA with the same normalization factor  $N$  for all states,  $\sigma_{\text{p.u.}} = N\sigma_{\text{DW}}$ , then we can estimate the compound nucleus and

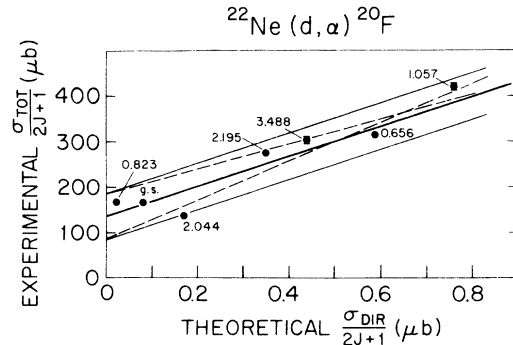


FIG. 4. Plot of the experimental total cross section  $\sigma_{\text{TOT}}/(2J+1)$  vs the predicted DWBA total cross sections  $\sigma_{\text{DIR}}/(2J+1)$  for selected states of known  $J^\pi$  that have previously been identified with shell-model states. Experimental and predicted cross sections are for the reaction  $^{22}\text{Ne}(d, \alpha)^{20}\text{F}$  at an incident energy of 10 MeV. The DWBA calculations are discussed in the text. The heavy solid line corresponds to the relation  $\sigma_{\text{TOT}}/(2J+1) = 137 + 330\sigma_{\text{DIR}}/(2J+1)$ , which corresponds to a compound-nucleus cross section constant  $\sigma_{\text{CN}} = 137(2J+1) \mu\text{b}$  and a DWBA normalization constant of  $N=330$ . The lighter solid lines correspond to values of 87 and 187 for the compound-nucleus cross section constant  $\sigma_{\text{CN}}$ , and the broken lines correspond to normalization factors of  $N=250$  and  $410$ .

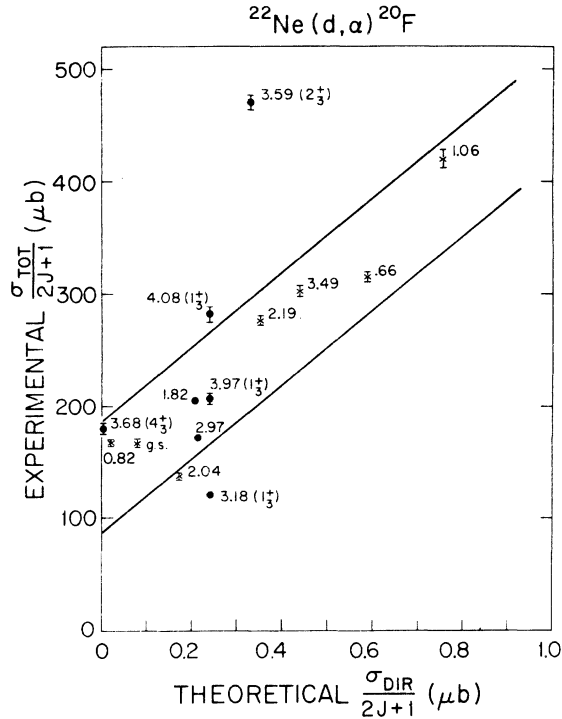


FIG. 5. Plot of  $\sigma_{\text{TOT}}/(2J+1)$  vs  $\sigma_{\text{DIR}}/(2J+1)$  for several states of  $^{20}\text{F}$  populated in the  $^{22}\text{Ne}(d, \alpha)^{20}\text{F}$  reaction. See caption of Fig. 4 for additional details of the layout of this figure. The states of known  $J^\pi$  for which shell-model correspondences are well established that were plotted in Fig. 4 are indicated by  $x$ 's in this figure. The other states shown by dots are discussed in the text. The solid lines correspond to a normalization constant,  $N = 330$  and  $\sigma_c = 87$  and  $187$ .

direct contributions for the various states. Restricting our attention to the states whose structure is rather well known,<sup>10</sup> we can use the measured cross section to estimate  $\sigma_c$  and  $N$ . This is done in Fig. 4, where  $\sigma_{\text{TOT}}/2J+1$  is plotted vs  $\sigma_{\text{DIR}}/2J+1$  for these states. Here  $\sigma_{\text{TOT}}$  is the measured quantity and  $\sigma_{\text{DIR}}$  is the predicted DWBA cross section. With our assumptions, we expect

$$\frac{\sigma_{\text{TOT}}}{2J+1} = \sigma_c + N \frac{\sigma_{\text{DIR}}}{2J+1},$$

so that the points in Fig. 4 should lie on a straight line with slope equal to  $N$  and  $y$  intercept equal to  $\sigma_c$ . The data follow a monotonic trend; all the data are consistent with the values  $\sigma_c = 137 \pm 50$   $\mu\text{b}$  and  $N = 330 \pm 80$ . This value of  $N$  is not unreasonable for a  $(d, \alpha)$  reaction.<sup>17</sup> Thus, it seems that several states have a measurable direct cross section. In the penultimate column of Table I, we have extracted the value of  $N$  for several states,

assuming that  $\sigma_{\text{CN}} = (2J+1)137$   $\mu\text{b}$ . For the states that are predicted to have a large pickup cross section, the values of  $N$  are surprisingly constant when compared with other two-nucleon transfer reactions. (See, e.g., Ref. 10.)

It is possible to extend these results to suggest shell-model states which can be associated with other experimental states of  $^{20}\text{F}$ . Such a procedure is highly model-dependent requiring that the shell model correctly reproduces the details of the corresponding nuclear state. Of course, this prescription apparently is capable of reproducing the total cross sections of the several states of known configuration discussed above.

In Fig. 5 the same quantity is plotted as in Fig. 4. The states that also are shown in Fig. 4 are plotted as crosses in Fig. 5, and several other states as dots. Several facts emerge. (1) The cross sections for doublets at 1.82 and 2.97 MeV imply that the negative-parity members of both doublets have small direct cross sections. (2) The cross section for the 3.68-MeV state is consistent with it being identified with the second  $4^+$  model state, which is predicted to have a small pickup cross section. (3) The cross section for the 3.97-MeV state is consistent with it being identified with the third  $1^+$  model state. The 3.18-MeV state (which also seems to have  $J=0$  or  $1$ ) is too weak to be the  $1_3^+$  model state. The 4.08-MeV  $1^+$  state is too strong to be the  $1_3^+$  model state. (4) The 3.59-MeV state is too strong to be identified with either the  $2_3^+$  or  $3_4^+$  model state. These results are summarized in the last two columns of Table I.

## SUMMARY

At a bombarding energy of 10.0 MeV, the  $^{22}\text{Ne}(d, \alpha)^{20}\text{F}$  reaction possesses a large compound-nucleus component for all final states. However, there appears to be a measurable direct-pickup cross section for those states of simple  $(sd)^4$  configuration that might be expected to be populated directly in this reaction. It would be interesting to compare these results with the results of a similar pickup experiment at much higher energies.

## ACKNOWLEDGMENTS

We thank B. H. Wildenthal for supplying us with his unpublished shell-model results for  $^{20}\text{F}$ , and for worthwhile discussions. We are grateful to V. Adams and L. Ballard for careful scanning of the nuclear track plates.

\*Work supported by the National Science Foundation.

†Present address: Niels Bohr Institute, University of Copenhagen, 2100 Copenhagen Ø, Denmark.

<sup>1</sup>R. Middleton, in *Proceedings of the International Conference on Nuclear Reactions Induced by Heavy-Ions, Heidelberg*, edited by R. Bock and W. R. Hering (North-Holland, Amsterdam, 1970), p. 263.

<sup>2</sup>R. Middleton, in *Proceedings of the Heavy Ion Summer Study, Oak Ridge National Laboratory, 1972* (Conf.-720669), edited by S. T. Thornton (available from National Technical Information Service, Springfield, Virginia, 1972), p. 315.

<sup>3</sup>M. A. Spivack, *Rev. Sci. Instrum.* **41**, 1614 (1970).

<sup>4</sup>J. D. Garrett, R. Middleton, D. J. Pullen, S. A. Andersen, O. Nathan, and O. Hansen, *Nucl. Phys. A164*, 449 (1971).

<sup>5</sup>F. Ajzenberg-Selove, *Nucl. Phys. A190*, 1 (1972) and references therein.

<sup>6</sup>H. T. Fortune, J. D. Garrett, P. Neogy, and R. Middleton, *Bull. Am. Phys. Soc.* **15**, 36 (1970).

<sup>7</sup>J. N. Bishop and H. T. Fortune, *Bull. Am. Phys. Soc.* **18**, 678 (1973); and (unpublished).

<sup>8</sup>See e.g. R. K. Sheline, H. L. Nielsen, and A. Sperduto, *Nucl. Phys.* **14**, 140 (1959); S. Hinds, R. Middleton, and A. E. Litherland, in *Proceedings of the Rutherford Jubilee International Conference, Manchester, 1961*, edited by J. B. Birks (Heywood and Co., Ltd., London,

1961), p. 305; O. Hansen, E. Koltay, N. Lund, and B. S. Madsen, *Nucl. Phys.* **51**, 307 (1964); N. MacDonald, *ibid.* **33**, 110 (1962).

<sup>9</sup>H. T. Fortune, G. C. Morrison, R. C. Barse, J. L. Yntema, and B. H. Wildenthal, *Phys. Rev. C* **6**, 21 (1972); and H. T. Fortune and R. R. Betts, *ibid.* **10**, 1292 (1974).

<sup>10</sup>D. J. Crozier and H. T. Fortune, *Phys. Rev. C* **10**, 1697 (1974).

<sup>11</sup>B. H. Wildenthal (unpublished).

<sup>12</sup>E. C. Halbert, J. B. McGrory, B. H. Wildenthal, and S. P. Pandya, in *Advances in Nuclear Physics*, edited by M. Baranger and E. Vogt (Plenum, New York, 1971), Vol. IV, p. 316.

<sup>13</sup>B. M. Freedom and B. H. Wildenthal, *Phys. Rev. C* **6**, 1633 (1972).

<sup>14</sup>P. D. Kunz, University of Colorado, Report No. C00-535-613 (unpublished).

<sup>15</sup>H. T. Fortune, T. J. Gray, W. Trost, and N. R. Fletcher, *Phys. Rev.* **179**, 1033 (1969).

<sup>16</sup>H. Kattenborn, C. Mayer-Boricke, and B. Mertens, *Nucl. Phys. A138*, 657 (1969); and J. D. Garrett, R. Middleton, and H. T. Fortune, *Phys. Rev. C* **2**, 1243 (1970); **4**, 1138 (1971).

<sup>17</sup>See, e.g., M. J. Schneider and J. W. Olness, *Phys. Rev. C* **13**, 1392 (1976).